
Article:
Tulotta, C., Lefley, D.V., Freeman, K. et al. (16 more authors) (2019) Endogenous production of IL-1B by breast cancer cells drives metastasis and colonisation of the bone microenvironment. Clinical Cancer Research, 25 (9). pp. 2769-2782. ISSN 1078-0432

https://doi.org/10.1158/1078-0432.CCR-18-2202

Endogenous production of IL-1B by breast cancer cells drives metastasis and colonisation of the bone microenvironment.

Claudia Tulotta[1], Diane V Lefley[1], Katy Freeman[1], Walter M Gregory[3], Andrew M Hanby[4], Paul R Heath[2], Faith Nutter[1], J Mark Wilkinson[1], Amy R Spicer-Hadlington[1], Xinming Liu[1], Steven M J Bradbury[1], Lisa Hambley[1], Victoria Cookson[1], Gloria Allocca[1] Marianna Kruithof de Julio[5], Robert E Coleman[1], Janet E Brown[1], Ingunn Holen[1], *Penelope D Ottewell[1].

[1]Department of Oncology and Metabolism, [2]Sheffield Institute for Translational Neuroscience, University of Sheffield, UK; [3]Leeds Institute of Clinical Trials Research, [4]Institute of Molecular Medicine, St James's University Hospital, Leeds, UK and [4]Department of Biomedical Research, University of Bern, Bern, Switzerland.

Corresponding author: Dr. Penelope Ottewell, Department of Oncology and Metabolism, Medical School, University of Sheffield, Beech Hill Road, Sheffield, S10 2RX, UK.

Telephone: +44 (0) 114 215 9058

E-Mail : p.d.ottewell@sheffield.ac.uk

Key words: Breast cancer, Bone metastasis, IL-1B, bone metastatic niche, biomarker, Canakinumab, IL-1R antagonist.

Running title: IL-1B promotes breast cancer bone metastasis

Conflicts of interest: IH has received speakers bureau support from Amgen. REC is Co-inventor and patent holder of a bone biomarker under development by Inbiomotion, has received fees for advising on clinical trial protocol development from Amgen, Astellas and Boehringer Ingelheim as well as for independent medical education lectures at symposia supported by Amgen, Genomic Health and Eisai. JEB has received fees for attendance at Advisory Boards for Amgen, Novartis, Bayer, Sandoz, Roche, BMS and Takeda and for Speaker Bureaux for Amgen and Novartis as well as travel funding to a scientific meeting from Ipsen. Institutional research funding has been received from Amgen and Bayer.

Funding: This work was funded by research grants from the Medical Research Council (MR/P000096/1), UK and Weston Park Cancer Charity (CA142).

Translational relevance

Our unique study using patient samples, humanised mouse models of bone metastasis, genetic manipulation of breast cancer cells and in vitro modelling demonstrate multiple roles for tumor cell-derived IL-1B in the process of breast cancer bone metastasis. These data are hugely significant to clinicians and basic scientists alike: Our results suggest that tumor-cell derived IL-1B can be used as a biomarker to predict patients who are likely to experience breast cancer relapse and metastasis. In addition, we provide evidence that targeting IL-1B signalling with the anti IL-1B antibody, Canakinumab, or the IL-1R antagonist, Anakinra, may provide therapeutic benefit to patients with tumors that express IL-1B specifically by the malignant cells. Future research will establish if tumor cell derived IL-1B can be used as a biomarker and therapeutic target for other cancers that metastasise to bone.

Abstract

***Background*:** Breast cancer bone metastases are incurable highlighting the need for new therapeutic targets. After colonizing bone, breast cancer cells remain dormant, until signals from the microenvironment stimulate outgrowth into overt metastases. Here we show that endogenous production of IL-1B by tumor cells drives metastasis and growth in bone.

Methods: Tumor/stromal IL-B and IL-1R1 expression was assessed in patient samples and effects of the IL-1R antagonist, Anakinra or the IL-1B antibody Canakinumab on tumor growth and spontaneous metastasis were measured in a humanized mouse model of breast cancer bone metastasis. Effects of tumor cell-derived IL-1B on bone colonisation and parameters associated with metastasis were measured in MDA-MB-231, MCF7 and T47D cells transfected with IL-1B/control.

Results: In tissue samples from >1300 patients with stage II/III breast cancer, IL-1B in tumor cells correlated with relapse in bone (hazard ratio 1.85; 95% CI 1.05-3.26; P=0.02) and other sites (hazard ratio 2.09; 95% CI 1.26-3.48; P=0.0016). In a humanized model of spontaneous breast cancer metastasis to bone, Anakinra or Canakinumab reduced metastasis and reduced the number of tumor cells shed into the circulation. Production of IL-1B by tumor cells promoted EMT (altered E-Cadherin, N-Cadherin and G-Catenin), invasion, migration and bone colonisation.
Contact between tumor and osteoblasts or bone marrow cells increased IL-1B secretion from all three cell types. IL-1B alone did not stimulate tumor cell proliferation. Instead, IL-1B caused expansion of the bone metastatic niche leading to tumor proliferation.

Conclusion: Pharmacological inhibition of IL-1B has potential as a novel treatment for breast cancer metastasis.

Introduction

There are over 508,000 deaths annually from breast cancer worldwide with around 75% of patients with advanced breast cancer developing bone metastasis (1). Although bone metastases are more common in oestrogen receptor (ER)+ve disease, ER –ve tumors also metastasise to the skeleton. Once breast cancer has spread to the bones, the disease is incurable and existing treatments can only slow progression. Median survival is 2-3 years following diagnosis of skeletal involvement, hence new therapeutic approaches are needed to improve outcome for these poor prognosis patients. (2). Identification of molecules that drive tumor growth in bone will provide targets for developing such urgently needed novel therapies. Elevated tumor IL-1B is associated with poor prognosis in a variety of cancers, including breast, prostate, colon, and lung (3). Importantly, recent data have demonstrated significantly reduced incidence of lung cancer in patients with atherosclerosis who have received the anti-Interleukin IB (IL-1B) antibody Canakinumab (4). However, the mechanisms by which IL-1B promotes cancer development and metastatic progression remains to be established.

We have recently identified a direct link between IL-1B and breast cancer bone metastasis (2): In a small study using a tissue array of 150 human primary breast cancer samples from patients with stage II/III breast cancer with a median follow up of 84 months (AZURE trial (5)) we found a significant correlation between IL-1B expression and subsequent development of bone metastases ($P < 0.0001$) (2). We have confirmed this link between IL-1B and breast cancer bone metastasis in animal models by demonstrating increased IL-1B expression in breast cancer cells that have been passaged *In viv*o to make them home to bone when injected directly into the blood stream (2). Our previously published data, therefore, suggest that IL-1B expressed by breast cancer cells makes them more aggressive and may play a role in the initiation of the metastatic process. IL-1B also appears to play a crucial role in the development of overt metastases from disseminated tumor cells within the bone environment: Inhibiting IL-1B binding to Interleukin 1 receptor 1 (IL-1R1) inhibits metastases from tumor cells disseminated in bone and reduces growth of established bone metastasis *in vivo* (6). These findings suggest that IL-1B also plays a role in the later stages of bone metastasis development in which breast cancer cells emerge from dormancy and proliferate in the bone microenvironment.

In the current study we have utilised *in vitro* and *in vivo* model systems in conjunction with patient samples to identify how tumor cell derived IL-1B drives the different

stages of breast cancer progression and bone metastasis. We have also investigated the effect of targeting the IL-1B pathway using compounds that are Food and Drug Administration (FDA) approved for the treatment of rheumatoid arthritis, using the anti-human IL-1B antibody Canakinumab (Canakinumab™) and IL-1R antagonist, Anakinra (Kineret™), on *in vivo* models of spontaneous human breast cancer metastasis to human bone implants, in order to establish the potential of repurposing these drugs for the treatment of breast cancer bone metastasis.

Materials and Methods

Experimental models and subject details

Animals

Experiments using human bone grafts were carried out in 10-week old female NOD SCID mice, IL-1B/IL-1R1 overexpression bone homing experiments used 6-8 week old female BALB/c nude mice, effects of IL-1B on the bone microenvironment used 10-week old female C57BL/6 mice (Charles River, Kent UK), IL-1R1 KO or IL-1B KO mice (7). Mice were maintained on a 12h: 12h light/dark cycle with free access to food and water. Experiments were carried out with home office approval under project licence 40/3531, University of Sheffield, UK.

Cell lines

Human breast cancer MDA-MB-231-Luc2-TdTomato (Calliper Life Sciences, Manchester UK), MDA-MB-231 (parental) MCF7, T47D (European Collection of Authenticated Cell Cultures (ECACC)), MDA-MB-231 IV (2) as well as E0771 mouse mammary cancer cells (ECACC) bone marrow HS5 (ECACC) and human primary PRE-osteoblasts, OB1, (gift from Dr Marianna de Julio) were cultured in DMEM + 10% FCS (Gibco, Invitrogen, Paisley, UK). Cell lines purchased from commercial sources have been authenticated in house using short tandem repeat analysis of 10 loci. All cell lines were cultured in a humidified incubator under 5% C02 and used at low passage >20 within 24 months of last date of authenification.

Patient samples

All human samples were obtained following written informed consent from patients and studies were conducted in accordance with the Declaration of Helsinki. IL-1B and IL-1R1 expression was assessed on tissue microarrays (TMA) containing primary breast tumor cores taken from 1,300 patients included in the clinical trial,

AZURE (Sponsored by the University of Sheffield and approved as a United Kingdom national trial by the Clinical Trials Committee; controlled trials number ISRCTN79831382) (5). These samples were taken from patients with stage II and III breast cancer, pre-treatment between 2003 and 2006, without evidence of metastasis. Patients were subsequently randomised to standard adjuvant therapy with or without the addition of zoledronic acid for 5 years and followed up for 10 years (5). The TMAs were stained for IL-1B and scored blindly, under the guidance of histopathologist, Prof. Andrew Hanby, for IL-1B/IL-1R1 in the tumor cells or in the associated stroma. Tumor cell or stromal IL-1B or IL-1R1 was then linked to disease recurrence (any site) or disease recurrence specifically in bone (+/- other sites).

Human bone

Human femoral bone was isolated from 60-70-year-old female patients who had undergone total hip replacement surgery for rheumatoid arthritis. Patients who had previous exposure to anti-resorptive drugs or anti-IL-1 treatments were excluded. All patients provided written, informed consent prior to participation in this study which was carried out in accordance with the ethical guidelines set out in the Declaration of Helsinki. Human bone samples were collected under Human Tissue Act (HTA) licence 12182, Sheffield Musculoskeletal Bio bank, University of Sheffield UK. Trabecular bone cores were prepared using an Isomet 4000 Precision saw (Buehler) with Precision diamond wafering blade (Buehler). 5mm diameter discs were subsequently cut using a bone trephine before storing in sterile PBS at ambient temperature.

Method details

Transfection of tumor cells:

Human MDA-MB-231, MCF 7 and T47D cells were stably transfected to over express IL-1B or IL-1R1 using plasmid DNA purified from competent *E.Coli* that have been transduced with an ORF plasmid containing human IL-1B or IL-1R1 (Accession numbers NM_000576 and NM_0008777.2 respectively) with a C terminal GFP tag (OriGene Technologies Inc. Rockville MD). Plasmid DNA purification was performed using a PureLink™ HiPure Plasmid Miniprep Kit (ThemoFisher) and DNA quantified by UV spectroscopy before being introduced into human cells with the aid of

Lipofectamine II (ThermoFisher). Control cells were transfected with DNA isolated from the same plasmid without IL-1B or IL-1R1 coding sequences.

***In vitro* studies**

In vitro studies were carried out with and without addition of 0-5ng/ml recombinant IL-1B (R&D systems, Wiesbaden, Germany) +/- 50uM IL-1Ra (Amgen, Cambridge, UK).

Cells were transferred into fresh media with 10% or 1% Foetal Calf Serum (FCS). Cell proliferation was monitored every 24h for up to 120h by manual cell counting using a $1/400^2$ haemocytometer (Hawkley, Lancing UK) or over a 72h period using an Xcelligence RTCA DP Instrument (Acea Biosciences inc). Tumor cell invasion was assessed using 6mm transwell plates with an 8uM pore size (Costar; Corning Incorporated, NY, USA) +/- basement membrane (20% Matrigel: Invitrogen). Tumor cells were seeded into the inner chamber at a density of $2.5X10^5$ for parental and MDA-MB-231 derivatives and $5X10^5$ for T47D in DMEM + 1% FCS and $5X10^5$ OB1 osteoblast cells supplemented with 5% FCS were added to the outer chamber. Cells were removed from the top surface of the membrane 24 and 48h after seeding and cells that had invaded through the pores were stained with haematoxylin and eosin before being imaged on a Leica DM7900 light microscope and manually counted.

Migration of cells was investigated by analysing wound closure: Cells were seeded onto 0.2% gelatine in 6-well tissue culture plates (Costar; corning incorporated); once confluent, 10ug/ml mitomycin C was added to inhibit cell proliferation and a 50uM scratch made across the monolayer. The percentage of wound closure was measured at 24 and 48h using a CTR7000 inverted microscope and LAS-AF v2.1.1 software (Leica Applications Suite; Leica Microsystems, Wetzlar, Germany). All proliferation, invasion and migration experiments were repeated using the Xcelligence RTCA DP instrument and RCTA Software (Acea, Biosystems inc).

For co-culture studies with human bone $5X10^5$ MDA-MB-231 or T47D cells were seeded onto tissue culture plastic or into $0.5cm^3$ human bone discs for 24h. Media was removed and analysed for concentration of IL-1B in the media by ELISA. For co-culture with HS5 or OB1 cells, $1X10^5$ MDA-MB-231 or T47D cells were cultured onto plastic along with $2X10^5$ HS5 or OB1 cells. Cells were sorted by FACS (as described below) 24h later counted and lysed for analysis of IL-1B concentration. Cells were collected, sorted and counted every 24h for 120h.

In vivo studies

To model human breast cancer metastasis to human bone implants; two-human bone discs were implanted subcutaneously into 10-week old female NOD SCID mice (n=10/group) under isofluorane anaesthetic. Mice received an injection of 0.003mg vetergesic and Septrin was added to the drinking water for 1-week following bone implantation. Mice were left for 4-weeks before injecting $1X10^5$ MDA-MB-231 Luc2-TdTomato, MCF7 Luc2 or T47D Luc2 cells in 20% Martigel/79% PBS/1% toluene blue into the two hind mammary fat pads. Primary tumor growth and development of metastases was monitored weekly using an IVIS (Luminol) system (Caliper Life Sciences) following sub-cutaneous injection of 30mg/ml D luciferin (Invitrogen). On termination of experiments mammary tumors, circulating tumor cells, serum and bone metastases were resected. RNA was processed for downstream analysis by real time PCR , cell lysates were taken for protein analysis and whole tissue for histology as previously described (2,8).

For therapeutic studies in NOD SCID mice, placebo (control), 1mg/mg/day IL-1Ra or 10mg/kg/14 days Canakinumab (Novartis Pharmaceuticals) were administered subcutaneously starting 7 days after injection of tumor cells. In BALB/c mice and C57BL/6 mice 1mg/kg/day IL-1Ra was administered for 21 or 31 days or 10mg/kg Canakinumab was administered as a single sub-cutaneous injection. Tumor cells, serum, and bone were subsequently resected for downstream analysis.

Bone metastases were investigated following injection of $5X10^5$ MDA-MB-231 GFP (control), MDA-MB-231 IV, MDA-MB-231 IL-1B+ or MDA-MB-231 IL-1R1+ cells into the lateral tail vein of 6-8 week old female BALB/c nude mice (n=12/group) or following intra-ductal injection of E0771 $1.25X10^5$ cells into the 4^{th} and 9^{th} mammary ducts of IL-1B-KO or fl/fl control mice. Tumor growth in bones and lungs was monitored weekly by GFP imaging in live animals. Mice were culled 28 days after tumor cell injection at which point hind limbs, lungs and serum were resected and processed for uCT, histology and ELISA analysis of bone turnover markers and circulating cytokines as previously described (6).

Isolation of circulating tumor cells

Whole blood was centrifuged at 10,000g for 5 minutes and the serum removed for ELISA assays. The cell pellet was re-suspended in 5ml of FSM lysis solution (Sigma-Aldrich, Pool, UK) to lyse red blood cells. Remaining cells were re-pelleted, washed 3-times in PBS and re-suspended in a solution of PBS/10% FCS. Samples from 10-mice per group were pooled prior to isolation of TdTomato positive tumor cells using a MoFlow High performance cell sorter (Beckman Coulter, Cambridge UK) with the

470nM laser line from a Coherent I-90C tenable argon ion (Coherent, Santa Clara, CA). For gene expression analysis: TdTomato fluorescence was detected by a 555LP dichroic long pass and a 580/30nm band pass filter. Acquisition and analysis of cells was performed using Summit 4.3 software. Following sorting cells were immediately placed in RNA protect cell reagent (Ambion, Paisley, Renfrew, UK) and stored at -80^{0}C before RNA extraction. For counting numbers of circulating tumor cells: TdTomato fluorescence was detected using a 561 nm laser and an YL1-A filter (585/16 emission filter). Acquisition and analysis of cells was performed using Attune NxT software.

Microcomputed tomography (uCT) imaging:

µCT analysis was carried out using a Skyscan 1172 x-ray-computed µCT scanner (Skyscan, Aartselar, Belgium) equipped with an x-ray tube (voltage, 49kV; current, 200uA) and a 0.5-mm aluminium filter. Pixel size was set to 5.86 µm and scanning initiated from the top of the proximal tibia as previously described (9,10).

Bone histology and measurement of tumor volume:

Bone tumor areas were measured on 3, non-serial, Haematoxylin and Eosin (H&E) stained, 5µM histological sections of decalcified tibiae per mouse using a Leica RMRB upright microscope and Osteomeasure software (Osteometrics inc. Dakota, USA) and a computerised image analysis system (9).

Western blotting:

Protein was extracted using a mammalian cell lysis kit (Sigma-Aldrich, Poole, UK). 30ug of protein was run on 4-15% precast polyacrylamide gels (BioRad, Watford, UK) and transferred onto an imibilon-P nitrocellulose membrane (Millipore). Nonspecific binding was blocked with 1% casein (Vector laboratories) before incubation with rabbit monoclonal antibodies to human N-Cadherin (D4R1H) 1:1000, E-Cadherin (24E10) 1:500 or Gamma Catenin (2303) 1:500 (Cell signalling) or mouse monoclonal GAPDH (ab8245) 1:1000 (AbCam, Cambridge UK) for 16h at 4^0 C. Secondary antibodies were anti-rabbit or anti-mouse horse radish peroxidase (HRP; 1:15,000) and HRP was detected with the Supersignal chemiluminescence detection kit (Pierce). Band quantification was carried out using Quantity Once software (BioRad) and normalised to GAPDH.

Gene analysis

Total RNA was extracted using TRI reagent before being reverse transcribed into cDNA using High-capacity RNA-to cDNA kit (Thermofisher). Relative mRNA expression of IL-1B (Hs02786624), IL-1R1 (Hs00174097), Caspase 1 (Hs00354836), IL1RN (Hs00893626), JUP (Hs00984034), N-Cadherin (Hs01566408) and E-Cadherin (Hs1013933) were compared with the housekeeping gene glyceraldehyde-3-phosphate dehydrogenase (GAPDH; Hs02786624) and assessed using an ABI 7900 PCR System (Perkin Elmer, Foster City, CA) and Taqman universal master mix (All reagents were purchased from Applied Biosystems via Thermofisher, UK)). Fold change in gene expression between treatment groups was analysed by inserting CT values into Data Assist V3.01 software (Applied Biosystems) and changes in gene expression were only analysed for genes with a CT value of ≤25.

Immunohistochemistry

Immunohistochemistry for the endothelial cells was performed using a mouse specific anti CD34 antibody (MCA1825-GA: 1:50 dilution; Serotec, Oxford, UK) followed by a biotin conjugated anti-rat secondary antibody (E0467 1:200) as previously described (Nutter et al, 2014). Two-non-serial sections per sample were scored prior to statistical analysis.TMAs were stained for IL-1B (ab2105, 1:200 dilution, Abcam) and IL-1R1 (ab59995, 1:25 dilution, Abcam) and scored blindly, , for IL-1B/IL-1R1 in the tumor cells or in the associated stroma. Tumor or stromal IL-1B or IL-1R1 was then linked to disease recurrence (any site) or disease recurrence specifically in bone (+/- other sites).

Biochemical analysis

Serum concentrations of TRACP-5b and P1NP were measured using commercially available ELISA kits: Mouse TRAP™ Assay and Rat/Mouse P1NP competitive immunoassay kit (immunodiagnostic systems). Concentrations of IL-1B were analysed in mouse bone marrow, human breast cancer cells and in co-culture systems using anti-mouse or anti-human Quantikine ELISA kits, as appropriate (R&D systems, Abingdon, UK) and manufacturer's instructions.

QUANTIFICATION AND STATISTICAL ANALYSIS

For experiments using non-clinical material group wise comparisons were carried out using one-way independent ANOVA with Turkey's multiple comparison test using GraphPad PRISM® software version 6.0. Statistical significance was defined as P less than or equal to 0.05. A Cox proportional hazards model, using the statistical

software, was used to investigate the effect of Il-1B in a multivariate model including number of involved lymph nodes, tumor grade, oestrogen-receptor status, tumor stage and type of planned systemic therapy (endocrine therapy, chemotherapy or both). Statistical significance was determined using 2-sided p-values <.05.

Results

The IL-1B pathway is upregulated during the process of human breast cancer metastasis to human bone.

A mouse model of spontaneous human breast cancer metastasis to human bone implants was utilised to investigate how the IL-1B pathway changes through the different stages of metastasis (11); supplementary figure 1). Using this model, the expression levels of genes associated with the IL-1B pathway increased in a stepwise manner at each stage of the metastatic process in both triple negative (MDA-MB-231) and ER+ve (T47D) breast cancer cells: Genes associated with the IL-1B signalling pathway (IL-1B, IL-1R1, Caspase 1 and IL-1R antagonist (IL-1Ra)) were expressed at very low levels in both MDA-MB-231 and T47D cells grown *in vitro* and expression of these genes were not altered in primary mammary tumors from the same cells that did not metastasise *in vivo* (figure 1a).

IL-1B, IL-1R1 and Caspase 1 were all significantly increased in mammary tumors that subsequently metastasised to human bone, compared with those that did not metastasise ($P < 0.01$ for both cell lines), leading to activation of IL-1B signalling as shown by ELISA for active 17KD IL-1B (figure 1b; supplementary figure 2). IL-1B gene expression increased in circulating tumor cells compared with metastatic mammary tumors ($P < 0.01$ for both cell lines). IL-1B ($P < 0.001$), IL-1R1 ($P < 0.01$), Caspase 1 ($P < 0.001$) and IL-1Ra ($P < 0.01$) were further increased in tumor cells isolated from metastases in human bone compared with their corresponding mammary tumors, leading to further production of IL-1B protein (figure 1; supplementary figure 2). These data suggest that IL-1B signalling may promote both initiation of metastasis from the primary site, as well as development of breast cancer metastases in bone.

Tumor-derived IL-1B promotes EMT and breast cancer metastasis.

Expression levels of genes associated with tumor cell adhesion and epithelial to mesenchymal transition (EMT) were significantly altered in primary tumors that

metastasised to bone compared with tumors that did not metastasise (figure 1c). We therefore generated IL-1B overexpressing cells (MDA-MB-231-IL-1B+, T47D-IL-1B+ and MCF7-IL-1B+) to investigate whether tumor cell-derived IL-1B is responsible for inducing EMT and metastasis to bone. Compared to the corresponding controls, all IL-1B+ cell lines demonstrated increased EMT, exhibiting morphological changes from an epithelial to mesenchymal phenotype (figure 2a) as well as reduced proliferation (figure 2b), reduced expression of E-cadherin, and Junction plakoglobin (JUP) and increased expression of N Cadherin gene and protein (figure 2c and d). Wound closure ($p < 0.0001$ in MDA-MB-231-IL-1B+; $p < 0.001$ MCF7-IL-1B+ and T47D-IL-1B+ (figure 2e)), migration and invasion through matrigel towards osteoblasts ($p < 0.0001$ in MDA-MB-231-IL-1B+; $p < 0.001$ MCF7-IL-1B+ and T47D-IL-1B+ (figure 2g)) were increased in tumor cells with elevated IL-1B signalling (IL-1B+) compared with their respective controls. These data imply that endogenous production of IL-1B by tumor cells promotes EMT and promotes a more invasive and migratory phenotype.

Inhibition of IL-1B signalling reduces spontaneous metastasis to human bone.

As tumor cell-derived IL-1B appeared to be promoting onset of metastasis through induction of EMT, we next investigated the effects of inhibiting IL-1B signalling with an IL-1 receptor antagonist (IL-1Ra) or the human antibody against IL-1B, Canakinumab, on primary tumor growth and spontaneous metastasis to human bone implants: Daily administration of IL-1Ra had no effect on growth of MDA-Td cells in the mammary fat pad, whereas fortnightly administration of Canakinumab resulted in significantly increased growth of the primary tumor ($P = 0.003$ compared with placebo and 0.006 compared with IL-1Ra; figure 3a). In contrast, both IL-1Ra and Canakinumab reduced metastasis to human bone; metastases were detected in human bone implants from 7/10 control mice, 4/10 IL-1Ra treated mice and 1/10 Canakinumab treated mice. Bone metastases isolated from IL-1Ra and Canakinumab treatment groups were also smaller than those detected in the control group (figure 3b) suggesting that specific inhibition of human IL-1B produced by the tumor cells reduces metastasis. Numbers of cells detected in the circulation of mice treated with Canakinumab or IL-1Ra were significantly lower than those detected in the placebo treated group: Only 3 tumor cells/ml were counted in whole blood from mice treated with either Canakinumab or IL-1Ra compared to 108 tumor cells/ml counted in blood from placebo treated mice (supplementary figure 4). These data suggest that inhibition of IL-1 signalling prevents tumor cells from being shed from the primary site into the circulation.

Tumor cell derived IL-1B promotes bone homing and colonisation of breast cancer cells.

To assess whether metastasis was driven by IL-1B from tumor cells or from the microenvironment, we used genetic manipulation to increase expression of IL-1B in tumor cells alongside a mouse model from which IL-1B has been genetically knocked out (IL-1B KO). Injection of breast cancer cells into the tail vein of mice usually results in lung metastasis due to tumor cells becoming trapped in the lung capillaries. We have previously shown that breast cancer cells that preferentially home to the bone microenvironment following intra-venous injection express high levels of IL-1B, suggesting that this cytokine may be involved in tissue-specific homing of breast cancer cells to bone (2). In the current study, intra-venous injection of MDA-MB-231-IL-1B+ cells into BALB/c nude mice resulted in significantly increased number of animals developing bone metastasis (75%) compared to animals injected with control cells (12%) ($P < 0.001$; figure 3c). MDA-MB-231-IL-1B+ tumors caused development of significantly larger osteolytic lesions in mouse bone compared with control cells ($P = 0.03$; figure 3d) There was a non-significant numerical reduction in lung metastases in mice injected with MDA-MB-231-IL-1B+ cells compared with control cells ($P = 0.16$; figure 3e). Removal of IL-1B from the microenvironment did not alter metastasis: Injection of E0771 cells into the mammary ducts of IL-1B KO and control (IL-1B fl/fl) mice resulted in metastasis in bone and lung (figure 3f). These data strengthen the hypothesis that endogenous IL-1B rather than Il-1B from the microenvironment promotes tumor cell homing and development of bone metastases..

Tumor cell-bone cell interactions further induce IL-1B and promote development of overt metastases.

Using assays specifically designed to amplify human mRNA, gene analysis data from our mouse model of human breast cancer metastasis to human bone implants suggested that the IL-1B pathway was further increased when breast cancer cells are growing in the bone environment compared with metastatic cells in the primary site or in the circulation (figure 1a). We therefore investigated how IL-1B production changes when tumor cells come into contact with bone cells and how IL-1B alters the bone microenvironment to affect tumor growth (figure 4). Culture of human breast cancer cells into pieces of whole human bone for 48h results in increased secretion of IL-1B into the media ($P < 0.0001$ for MDA-MB-231 and T47D cells; figure 5a). Co-culture with human HS5 bone marrow cells revealed that increased IL-1B

concentrations originated from both the cancer cells ($P < 0.001$) and bone marrow cells ($P < 0.001$), with IL-1B from tumor cells increasing ~1000 fold and IL-1B from HS5 cells increasing ~100 fold following co-culture (figure 4b).

It is hypothesised that when metastatic tumor cells arrive in the bone they either reside in the vascular niche from which they may be stimulated to form overt metastasis through expansion of the associated vasculature or they are deposited in the bone marrow from which they home to the osteoblastic niche and become dormant (12-15). Stimulation of osteoblast proliferation is thought to stimulate proliferation of previously dormant tumor cells within this niche, thereby promoting onset of overt metastases (8,12,16). We therefore investigated the effects of exogenous IL-1B and IL-1B from tumor cells on proliferation of tumor cells, osteoblasts and bone marrow cells as well as the effects of IL-1B on CD34+ blood vessels: Co-culture of HS5 bone marrow or OB1 primary osteoblast cells with breast cancer cells caused increased proliferation of all cell types ($P< 0.001$ for HS5, MDA-MB-231 or T47D, figure 4c) ($P < 0.001$ for OB1, MDA-MB-231 or T47D, figure 4d). Furthermore, administration of IL-1B increased proliferation of HS5 (figure 5b) or OB1 (figure 5c) cells but not breast cancer cells (figure 5a), suggesting that tumor cell-bone cell interactions promote production of IL-1B that can drive expansion of the niche and stimulate the formation of overt metastases.

IL-1B signalling was also found to have significant effects on the bone microvasculature: Preventing IL-1B signalling in bone by knocking out IL-1R1, pharmacological blockade of IL-1R with IL-1Ra or reducing circulating concentrations by administration of an anti-IL-1B antibody reduced the average length of CD34+ blood vessels in trabecular bone, where tumor colonisation takes place (Wang et al 2014) ($P < 0.01$ for IL-1Ra and anti-IL-1B treated mice) (figure 5c). These findings were confirmed by endomeucin staining which showed decreased numbers of blood vessels and blood vessels length in bone when IL-1B signalling was disrupted (data not shown). ELISA analysis for endothelin 1 and VEGF showed reduced concentrations of both of these endothelial cell markers in the bone marrow in IL-1R1 KO mice ($P < 0.001$ endothelin 1; $P < 0.001$ VEGF), mice and mice treated with IL-1R antagonist ($P < 0.01$ endothlin 1; $P < 0.01$ VEGF) or Canakinumab ($P < 0.01$ endothelin 1; $P < 0.001$ VEGF) compared with control (supplementary figure 5). These data suggest that tumor cell-bone cell associated increases in IL-1B and high levels of IL-1B in tumor cells may also promote angiogenesis, further stimulating metastases.

IL-1B promotes osteoclast and osteoblast activity *in vivo.*

High levels of bone turnover are associated with increased bone metastasis and It is hypothesised that interactions between tumor cells and bone cells instigate a vicious cycle whereby tumor cells stimulate osteoclast activity and bone resorption. Subsequent release of growth factors from the bone then stimulates growth of tumor cells (17). Bone turnover is primarily regulated by activity of osteoclast and osteoblasts, we therefore investigated the effects of IL-1B signalling on activity of these cell types (supplementary figure 6). Mice that are globally deficient in IL-1R1 have significantly increased trabecular bone volume ($P < 0.0001$; Supplementary figure 6a), decreased osteoclast activity ($P<0.0001$) and decreased osteoblast activity ($P<0.0001$) compared with control (IL-1R1 fl/fl) mice (supplementary figure 6b). Disrupting IL-1B signalling by daily injection with 1mg/kg IL-1Ra or Canakinumab every 14 days for 8 weeks in mice bearing human bone implants also led to reduced osteoclast ($P<0.001$ for IL-1Ra and $P< 0.01$ for Canakinumab) and osteoblast ($P<0.0001$ for IL-1Ra and $P<0.001$ for Canakinumab) activity (supplementary figure 6c). Interestingly, growing tumor cells that express high levels of IL-1B in mouse bone (MDA-MB-231-IL-1B+) resulted in increased osteoclast activity ($P< 0.01$) compared with control cells growing in the same environment but osteoblast activity was not altered (supplementary figure 6d). These data indicate that IL-1B has profound effects on osteoclast and osteoblast activity *in vivo* and inhibiting bone turnover through anti-IL-1 treatments may be a mechanism by which this therapeutic approach reduces bone metastases.

Tumor cell derived IL-1B predicts future breast cancer relapse in bone and other organs in clinical samples

To establish the relevance of our laboratory findings in a clinical setting we investigated the correlation between IL-1B and its receptor IL-1R1 in patient samples. 1189 primary tumor samples (not previously included in our hypothesis generating study (2)) from patients with stage II/III breast cancer with no evidence of metastasis included in the randomized phase III AZURE trial evaluating standard adjuvant systemic therapy with or without the bisphosphonate, zoledronic acid (18) were stained for the 17KD form of active IL-1B or IL-1R1. Samples were scored separately for expression of IL-1B or IL-1R1 in the tumor cells and the tumor associated stroma. Patents were followed up for 10-years and correlation between IL-1B/IL-1R1 expression and distant recurrence or relapse in bone assessed using a Cox proportionate hazards model. IL-1B in tumor cells strongly correlated with distant

recurrence at any site (P = 0.0016: Hazard ratio 2.09; CI 1.26-3.48) or recurrence in bone at any time (P = 0.0387: Hazard ratio 1.85: CI 1.05-3.26) (figure 6). IL-1B in the stroma did not correlate with future relapse nor did IL-1R1 in the tumor or the stroma (supplementary table 1). Patients who had IL-1B in their tumor cells and IL-1R1 in the tumor associated stroma were more likely to experience future relapse at a distant site (P = 0.042), compared to patients who did not have IL-1B in their tumor cells, indicating that tumor-derived IL-1B may not only promote metastasis directly but also interact with IL-1R1 in the stroma to promote this process.

Bone metastases are more prevalent in ER+ve breast cancer whereas, ER-ve tumors are more likely to metastasise to lung. To investigate the prognostic value of IL-1B in different patient sub-groups, we analysed the correlation between IL-1B in tumor cells and future relapse in bone or any tissue for ER+ve and ER-ve tumors separately. The link between IL-1B and bone metastasis was significantly stronger in ER+ve tumors (p= 0.02: Hazard ratio 2.09: CI 1.11-3.83) than in ER-ve tumors (p=0.65: Hazard ratio 0.71: CI 0.16-3.09). However, no differences were observed between IL-1B expression in tumor cells and recurrence at any site between patients with ER+ve and ER-ve disease. Both groups showed a strong positive correlation with IL-1B in tumor cells and subsequent distal metastases (Hazard ratios 2.05 for ER+ve and 2.21 for ER-ve, respectively). Taken together these data suggest that expression of IL-1B by tumor cells is predictive of future development of metastases.

Discussion

Our data show that endogenous production of IL-1B by breast cancer cells increases their metastatic potential in *in vitro* and *in vivo* models and is associated with increased bone recurrence in breast cancer patients. Increased IL-1B production was seen in ER+ve and ER-ve breast cancer cells that spontaneously metastasised to human bone implants *in vivo* compared with non-metastatic breast cancer cells (figure1). The same link between IL-1B and metastasis was made in primary tumor samples from patients with stage II and III breast cancer enrolled in the AZURE study (18) that experienced disease recurrence during a 10 year follow-up period. In a previous study we have shown a link between IL-1B in primary tumor samples and subsequent relapse in bone from 150 samples over a 5-year follow up period (2). In the current study we were interested in assessing whether this correlation was associated specifically with IL-1B produced by tumor cells or IL-1B from the tumor environment. We therefore used an antibody to the active 17KD form of IL-1B and

scored IL-1B in tumor cells and the stoma separately. Interestingly, expression of IL-1B in tumor cells correlated with both relapse in bone and relapse at any site indicating that presence of this molecule is likely to play a role in metastasis in general. No correlation was observed between IL-1B in the tumor microenvironment or IL-1R1 expression, indicating that relapse in distant organs is influenced by tumor-cell derived IL-1B. Further analysis revealed that correlation between IL-1B expression in tumor cells and subsequent recurrence specifically in bone is highly significant in patients with ER+ve tumors ($P < 0.02$), but this correlation was not observed in patients with ER-ve disease. In contrast, expression of IL-1B in primary tumor samples was predictive of distal recurrence to any site in both ER+ve and ER-ve disease. Bone metastases are more common from ER+ve tumors and in our data set of 1189 patients bone metastasis developed from 181 ER+ve tumors and 29 ER-ve tumors. It is therefore likely that lack of correlation between IL-1B and bone metastasis, observed in the ER-ve group, is due to the small number of patients in this group providing insufficient power for these calculations. A larger set of patients is required to test this hypothesis

In agreement with the clinical data, genetic manipulation of breast cancer cells to artificially overexpress IL-1B increased their migration and invasion capacities *in vitro* (figure 2). Furthermore, inhibition of IL-1B signalling with the human specific anti-IL-1B antibody Canakinumab or inhibition of the IL-1R reduced the number of breast cancer cells shed into the circulation and reduced metastases in human bone implants (figure 3). Interestingly, administration of Canakinumab significantly increased growth of MDA-Td cells in the mammary fat pad whereas the IL-1Ra had no effect. Daily administration of IL-1Ra has previously been shown to reduce sub-cutaneous tumor growth of MDA-IV and MCF7 cells (6) as well as causing a small reduction in growth of 4T1 cells injected into the mammary fat pad (6,19). Data from both of these studies suggest that inhibition of IL-1 does not exert direct cytotoxic effects on tumor cells, but inhibits tumor cell proliferation possibly by inhibiting the formation of new blood vessels (6,19). In the current study both control and IL-1Ra treated tumors were small ($>0.3mm^3$) when mice were culled and therefore it is likely that tumors were too small for differences in growth to be detected (figure 3a). Until now there have been no reports on the effects of Canakinumab on tumor growth and metastasis. Data from patients with atherosclerosis who have received Canakinumab demonstrate significantly reduced incidences of lung cancer, however, the study was not designed to investigate effects on existing cancer (4). Canakinumab is an antibody that specifically targets IL-1B whereas the IL-1Ra inhibits both IL-1B and IL-

1A, suggesting that IL-1A may play a role in growth of the primary tumor whereas IL-1B is more prominent in driving the metastatic process.

Previous reports have focused on the role of exogenous IL-1B in progression of metastasis. Adding IL-1B to MCF7 cells in culture in the presence of EGF or TNFa1 to MCF7 has been shown to promote EMT related changes the actin cytoskeleton (20,21) and induces an invasive phenotype (22). Our data are in agreement with these findings; tumor cells overexpressing IL-1B and IL-1R1 overexpressing cells stimulated with IL-1B have a more mesenchymal phenotype and exhibit molecular changes associated with EMT including reduced JUP; a molecule whose reduction is strongly associated with tumor cell shedding into the blood (23) (figure 2). However, we also show that in order to generate pro-metastatic effects, significantly higher doses of exogenous IL-1B are required to achieve the same pro-migratory effects, as endogenous IL-1B (5ng/ml of exogenous IL-1B exerts similar invasive and migratory effects as 10-20pg/ml tumor derived IL-1B, supplementary figure 3), suggesting that IL-1B produced by the tumor cells is a more potent inducer of metastasis than exogenous sources. Spread of metastatic E0771 tumor cells from the primary site to bone or lung occurs in both IL-1B KO and control animals (figure 3f). These data, taken with the absence of a correlation between IL-1R1 in tumor cells with distant recurrence at any site (supplementary table 1) further imply that metastasis is stimulated by endogenous IL-1B from the tumor cells rather than exogenous sources of IL-1B acting upon the tumor cells.

Recent work has demonstrated that IL-1B promotes IL17 expression from YδT cells causing expansion and polarisation of neutrophils in mammary tumors that in turn promotes metastasis (24). The authors hypothesised that IL-1B secreted from macrophages within the tumor is likely to be the key driver of this process. Canakinumab does not cross react with mouse IL-1B, and our *in vivo* models do not express T cells, therefore, although IL-1B positive neutrophils are likely to be an important tumor promoter, it is clear that tumor derived IL-1B also plays a key role in driving the metastatic process. Retrospective analysis of our data show that IL-1B positive immune cells were present at very low numbers in our patient samples and therefore it was not possible for us to investigate this hypothesis. However, patients who have IL-1B in their primary tumors and IL-1R1 in their tumor-associated stroma had increased breast cancer recurrence at distant sites. It is therefore likely that as well as promoting EMT, IL-1B from tumor cells interacts with cells from the local environment, including immune cells, promoting a metastasis-inducing environment.

Once tumor cells leave their primary site they home to secondary metastatic organs. In breast cancer these are primarily bone, lung, and brain with bone being the most prominent (7). We have previously shown that a bone seeking breast cancer cell line, (MDA-IV) produces high concentrations of IL-1B compared to parental MDA-MB-231 cells (2). Similarly, in a PC3 model of prostate cancer genetic overexpression of IL-1B increased bone metastases from tumor cells injected into the heart whereas genetic knockdown of this molecule reduced bone metastasis (25). In keeping with this, our current study shows that breast cancer cells engineered to overexpress IL-1B (MDA-MB-231-IL-1B+) have increased bone homing capabilities. Importantly, all of the models described above have been designed to investigate bone metastasis and although our data show a strong link between IL-1B expression and bone homing, it does not exclude IL-1B involvement in metastasis to other sites.

Bone metastases occur when tumor cells are disseminated into the bone marrow and take up residence in the bone metastatic niche. This niche is thought to be made up of three interacting niches, the osteoblastic, vascular and hematopoietic stem cell niche (reviewed by (26,27)). There is increasing evidence from patient samples and model systems showing that stimulation of bone turnover and expansion of the bone metastatic niche promotes metastasis (8,12,13,16,28). Evidence for metastases in other organs predicts that proliferation of vascular endothelial cells and sprouting of new blood vessels may also promote proliferation of tumor cells in bone driving metastases formation (14,15,29). We have previously shown that inhibiting IL-1R signalling with the IL-1R antagonist Anakinra prevents formation of overt metastasis from MDA-IV cells disseminated in bone by maintaining these cells in a state of dormancy (6). Recent evidence from mouse models of prostate cancer has also shown reduced bone metastasis from androgen receptor positive prostate cancer cells disseminated in bone following administration of Anakinra (30). Shahriari *et al.* demonstrated that IL-1b secreted by prostate cancer cells generated cancer associated fibroblasts (CAFs) in the skeleton via upregulation of S100A4 and COX2 (30). We have also demonstrated increased S100A4 in IL-1B overexpressing MDA IV breast cancer cells (2) and it is highly likely that IL-1B produced by tumor cells induces changes in mesenchymal stem cells leading to the generation of CAFs that in turn provide a supportive environment for the growth of cancer cells in bone. Our new data clearly show that anti-metastatic effects of Anakinra are not just due to reductions in CAFs but are due to inhibition of the activity of IL-1B on the bone metastatic niche. Inhibition of IL-1 signalling by treatments with Canakinumab, IL-1Ra or genetic knock out of IL-1R1 *in vivo* reduced bone turnover and reduced blood

vessel length in the area of bone most commonly colonized by breast cancer cells (the trabecular region of the metaphysis) (12). This decreased blood vessel length is associated with decreased concentrations of endothelial cell growth factors endothelin 1 and VEGF (supplementary figure 3). Therefore inhibiting IL-1B signalling may also reduce expansion of the metastatic niche by inhibiting neo-vascularisation (31-33). We established that direct contact between tumor cells, primary human bone samples, bone marrow cells or osteoblasts promoted release of IL-1B from both tumor and bone cells (figure 4). Exogenous IL-1B did not increase tumor cell proliferation, even in cells overexpressing IL-1R1 (data not shown). Instead, IL-1B stimulated proliferation of bone marrow cells, osteoblasts and blood vessels induced proliferation of tumor cells (figure 4). It is therefore likely that arrival of tumor cells expressing high concentrations of IL-1B will stimulate expansion of metastatic niche components and that contact between IL-1B expressing tumor cells and osteoblasts/blood vessels will drive tumor colonisation of bone.

It is hypothesized that stimulation of osteoclast activity leading to increased bone resorption results in the release of growth factors into the local environment that in turn stimulates tumor growth (17). *In vitro* studies have previously reported that exposure of osteoclasts to IL-1B stimulates osteoclastogenesis (34) and our new data confirm that this also occurs *in vivo* (supplementary figure 6). Removal of IL-1B signalling in IL-1R1 KO mice or pharmacological inhibition of IL-1 signalling with IL-1Ra or Canakinumab significantly reduces osteoclast activity. Interestingly, Canakinumab reduced osteoclast and osteoblast activity in mice bearing human bone implants, albeit to a lesser degree than Anakinra. Whether these effects are due to altered activity of osteoblasts and osteoclasts specifically in the human bone implants or direct effects of this human specific antibody on mouse bone remains to be established. Taken together, our data suggest that in addition to other mechanisms, IL-1B stimulated by tumor cell/bone cell interactions promotes osteoclast activity driving tumor progression at this site. Hence, inhibiting IL-1B reduces bone metastases by blocking this process.

In conclusion, our data show that IL-1B is a novel biomarker that can be used to predict risk of breast cancer relapse. IL-1B activates different pro-metastatic mechanisms at the primary site compared with the metastatic site: Endogenous production of IL-1B by breast cancer cells promotes EMT, invasion, migration and organ specific homing. Once tumor cells arrive in the bone environment, contact between tumor cells and osteoblasts or bone marrow cells increased IL-1B secretion from all three-cell types. These high concentrations of IL-1B caused proliferation of

the bone metastatic niche and increased osteoclastic bone resorption stimulating growth of disseminated tumor cells into overt metastases (see supplementary figure 7). These pro-metastatic processes were inhibited by administration of anti-IL-1B treatments. Therefore, targeting IL-1B with Canakinumab or an IL-1Ra may represent a novel therapeutic approach for breast cancer patients at risk of progressing to metastasis by preventing seeding of new metastases from established tumors and retaining tumor cells already disseminated in the bone in a state of dormancy.

Acknowledgements : The authors would like to thank the ECMC for supporting retrieval of clinical samples from the AZURE trial; Breast Cancer Now for supporting the salary of Dr Victoria Cookson ; Weston Park Cancer Charity for supporting technical input from Mrs Alyson Evans and Yorkshire Cancer Research for purchase of the IVIS imaging machine. We would also like to thank Professor Sheila Francis, University of Sheffield and Dr Emmanuel Pinteaux, University of Manchester for supplying the IL-1R1 knockout mice.

Author contributions : CT, performed and analysed in vivo experiments looking at effects of Anakinra and Canakinumab on metastasis to human bone and effects of stable transfection of IL-1B on bone homing and metastasis. DVL, investigated the effects of tumor cell-derived IL-1B on EMT and was first scorer of IL-1B expression in tissue arrays. KF, acted as second scorer to validate IL-1B expression in tissue arrays. WG, performed statistical analysis on tissue arrays from the AZURE study. AH, provided training and expert guidance on scoring of tissue arrays. PRH, performed genetic analysis on primary, CTCs and bone metastatic tumors from the humanised model of bone metastasis. FN, performed original experiments using the humanised model of bone metastasis in which IL-1B was identified as a key driver in bone metastasis, JMW, provided human bone specimens for in vitro and in vivo experiments. ASH, performed uCT analysis on bones. XL, performed co-culture experiments and experiments involving addition of exogenous IL-1B in vitro. SB, carried out analysis of gene expression data under the guidance of PH and contributed to in vitro studies. LH, investigated the effects of IL-1B inhibition of the blood vessels. VC, performed transfection of breast cancer cell lines. MJK, produced the primary pre-osteoblast cells. REC, was principle investigator on the AZURE study and provided the tissue arrays. JEB, provided guidance on analysis of patient samples. IH, has had constant academic input into this project from the beginning and has contributed to writing this manuscript. PDO has been responsible for

overseeing this project, has carried out in vivo experiments, designed the majority of the experiments, checked data analysis and written the manuscript.

References

1. Coleman MP, Quaresma M, Berrino F, Lutz JM, De Angelis R, Capocaccia R*, et al.* Cancer survival in five continents: a worldwide population-based study (CONCORD). Lancet Oncol **2008**;9(8):730-56 doi 10.1016/S1470-2045(08)70179-7.
2. Nutter F, Holen I, Brown HK, Cross SS, Evans CA, Walker M*, et al.* Different molecular profiles are associated with breast cancer cell homing compared with colonisation of bone: evidence using a novel bone-seeking cell line. Endocr Relat Cancer **2014**;21(2):327-41 doi 10.1530/ERC-13-0158.
3. Lewis AM, Varghese S, Xu H, Alexander HR. Interleukin-1 and cancer progression: the emerging role of interleukin-1 receptor antagonist as a novel therapeutic agent in cancer treatment. J Transl Med **2006**;4:48 doi 10.1186/1479-5876-4-48.
4. Ridker PM, MacFadyen JG, Thuren T, Everett BM, Libby P, Glynn RJ*, et al.* Effect of interleukin-1beta inhibition with canakinumab on incident lung cancer in patients with atherosclerosis: exploratory results from a randomised, double-blind, placebo-controlled trial. Lancet **2017**;390(10105):1833-42 doi 10.1016/S0140-6736(17)32247-X.
5. Coleman R, Cameron D, Dodwell D, Bell R, Wilson C, Rathbone E*, et al.* Adjuvant zoledronic acid in patients with early breast cancer: final efficacy analysis of the AZURE (BIG 01/04) randomised open-label phase 3 trial. Lancet Oncol **2014**;15(9):997-1006 doi 10.1016/S1470-2045(14)70302-X.
6. Holen I, Lefley DV, Francis SE, Rennicks S, Bradbury S, Coleman RE*, et al.* IL-1 drives breast cancer growth and bone metastasis in vivo. Oncotarget **2016**;7(46):75571-84 doi 10.18632/oncotarget.12289.
7. Abdulaal WH, Walker CR, Costello R, Redondo-Castro E, Mufazalov IA, Papaemmanouil A*, et al.* Characterization of a conditional interleukin-1 receptor 1 mouse mutant using the Cre/LoxP system. Eur J Immunol **2016**;46(4):912-8 doi 10.1002/eji.201546075.
8. Ottewell PD, Wang N, Brown HK, Reeves KJ, Fowles CA, Croucher PI*, et al.* Zoledronic acid has differential antitumor activity in the pre- and postmenopausal bone microenvironment in vivo. Clin Cancer Res **2014**;20(11):2922-32 doi 10.1158/1078-0432.CCR-13-1246.
9. Ottewell PD, Deux B, Monkkonen H, Cross S, Coleman RE, Clezardin P*, et al.* Differential effect of doxorubicin and zoledronic acid on intraosseous versus

extraosseous breast tumor growth in vivo. Clin Cancer Res **2008**;14(14):4658-66 doi 10.1158/1078-0432.CCR-07-1545.
10. Ottewell PD, Monkkonen H, Jones M, Lefley DV, Coleman RE, Holen I. Antitumor effects of doxorubicin followed by zoledronic acid in a mouse model of breast cancer. J Natl Cancer Inst **2008**;100(16):1167-78 doi 10.1093/jnci/djn240.
11. Wright LE, Ottewell PD, Rucci N, Peyruchaud O, Pagnotti GM, Chiechi A*, et al.* Murine models of breast cancer bone metastasis. BoneKEy reports **2016**;5:804 doi 10.1038/bonekey.2016.31.
12. Wang N, Docherty FE, Brown HK, Reeves KJ, Fowles AC, Ottewell PD*, et al.* Prostate cancer cells preferentially home to osteoblast-rich areas in the early stages of bone metastasis: evidence from in vivo models. J Bone Miner Res **2014**;29(12):2688-96 doi 10.1002/jbmr.2300.
13. Pedersen EA, Shiozawa Y, Pienta KJ, Taichman RS. The prostate cancer bone marrow niche: more than just 'fertile soil'. Asian J Androl **2012**;14(3):423-7 doi 10.1038/aja.2011.164.
14. Kienast Y, von Baumgarten L, Fuhrmann M, Klinkert WE, Goldbrunner R, Herms J*, et al.* Real-time imaging reveals the single steps of brain metastasis formation. Nat Med **2010**;16(1):116-22 doi 10.1038/nm.2072.
15. Carbonell WS, Ansorge O, Sibson N, Muschel R. The vascular basement membrane as "soil" in brain metastasis. PLoS One **2009**;4(6):e5857 doi 10.1371/journal.pone.0005857.
16. Ottewell PD, Wang N, Meek J, Fowles CA, Croucher PI, Eaton CL*, et al.* Castration-induced bone loss triggers growth of disseminated prostate cancer cells in bone. Endocr Relat Cancer **2014**;21(5):769-81 doi 10.1530/ERC-14-0199.
17. Maurizi A, Rucci N. The Osteoclast in Bone Metastasis: Player and Target. Cancers **2018**;10(7) doi 10.3390/cancers10070218.
18. Coleman RE, Marshall H, Cameron D, Dodwell D, Burkinshaw R, Keane M*, et al.* Breast-cancer adjuvant therapy with zoledronic acid. N Engl J Med **2011**;365(15):1396-405 doi 10.1056/NEJMoa1105195.
19. Bunt SK, Yang L, Sinha P, Clements VK, Leips J, Ostrand-Rosenberg S. Reduced inflammation in the tumor microenvironment delays the accumulation of myeloid-derived suppressor cells and limits tumor progression. Cancer Res **2007**;67(20):10019-26 doi 10.1158/0008-5472.CAN-07-2354.
20. Ma L, Lan F, Zheng Z, Xie F, Wang L, Liu W*, et al.* Epidermal growth factor (EGF) and interleukin (IL)-1beta synergistically promote ERK1/2-mediated invasive breast ductal cancer cell migration and invasion. Mol Cancer **2012**;11:79 doi 10.1186/1476-4598-11-79.

21. Soria G, Ofri-Shahak M, Haas I, Yaal-Hahoshen N, Leider-Trejo L, Leibovich-Rivkin T*, et al.* Inflammatory mediators in breast cancer: coordinated expression of TNFalpha & IL-1beta with CCL2 & CCL5 and effects on epithelial-to-mesenchymal transition. BMC Cancer **2011**;11:130 doi 10.1186/1471-2407-11-130.
22. Franco-Barraza J, Valdivia-Silva JE, Zamudio-Meza H, Castillo A, Garcia-Zepeda EA, Benitez-Bribiesca L*, et al.* Actin cytoskeleton participation in the onset of IL-1beta induction of an invasive mesenchymal-like phenotype in epithelial MCF-7 cells. Arch Med Res **2010**;41(3):170-81 doi 10.1016/j.arcmed.2010.04.010.
23. Holen I, Whitworth J, Nutter F, Evans A, Brown HK, Lefley DV*, et al.* Loss of plakoglobin promotes decreased cell-cell contact, increased invasion, and breast cancer cell dissemination in vivo. Breast Cancer Res **2012**;14(3):R86 doi 10.1186/bcr3201.
24. Coffelt SB, Kersten K, Doornebal CW, Weiden J, Vrijland K, Hau CS*, et al.* IL-17-producing gammadelta T cells and neutrophils conspire to promote breast cancer metastasis. Nature **2015**;522(7556):345-8 doi 10.1038/nature14282.
25. Liu Q, Russell MR, Shahriari K, Jernigan DL, Lioni MI, Garcia FU*, et al.* Interleukin-1beta promotes skeletal colonization and progression of metastatic prostate cancer cells with neuroendocrine features. Cancer Res **2013**;73(11):3297-305 doi 10.1158/0008-5472.CAN-12-3970.
26. Weilbaecher KN, Guise TA, McCauley LK. Cancer to bone: a fatal attraction. Nat Rev Cancer **2011**;11(6):411-25 doi 10.1038/nrc3055.
27. Massague J, Obenauf AC. Metastatic colonization by circulating tumour cells. Nature **2016**;529(7586):298-306 doi 10.1038/nature17038.
28. Westbrook JA, Cairns DA, Peng J, Speirs V, Hanby AM, Holen I*, et al.* CAPG and GIPC1: Breast Cancer Biomarkers for Bone Metastasis Development and Treatment. J Natl Cancer Inst **2016**;108(4) doi 10.1093/jnci/djv360.
29. Ghajar CM, Peinado H, Mori H, Matei IR, Evason KJ, Brazier H*, et al.* The perivascular niche regulates breast tumour dormancy. Nat Cell Biol **2013**;15(7):807-17 doi 10.1038/ncb2767.
30. Shahriari K, Shen F, Worrede-Mahdi A, Liu Q, Gong Y, Garcia FU*, et al.* Cooperation among heterogeneous prostate cancer cells in the bone metastatic niche. Oncogene **2017**;36(20):2846-56 doi 10.1038/onc.2016.436.
31. Bagnato A, Rosano L. The endothelin axis in cancer. Int J Biochem Cell Biol **2008**;40(8):1443-51 doi 10.1016/j.biocel.2008.01.022.
32. Bachelier R, Confavreux CB, Peyruchaud O, Croset M, Goehrig D, van der Pluijm G*, et al.* Combination of anti-angiogenic therapies reduces osteolysis and

tumor burden in experimental breast cancer bone metastasis. Int J Cancer **2014**;135(6):1319-29 doi 10.1002/ijc.28787.
33. Semesiuk NI, Zhylchuk A, Bezdenezhnykh N, Lykhova A, Vorontsova AL, Zhylchuk VE*, et al.* Disseminated tumor cells and enhanced level of some cytokines in bone marrow and peripheral blood of breast cancer patients as predictive factors of tumor progression. Exp Oncol **2013**;35(4):295-302.
34. Lee WS, Lee EG, Sung MS, Yoo WH. Kaempferol inhibits IL-1beta-stimulated, RANKL-mediated osteoclastogenesis via downregulation of MAPKs, c-Fos, and NFATc1. Inflammation **2014**;37(4):1221-30 doi 10.1007/s10753-014-9849-6.

Figure 1. *In vivo* model of spontaneous human breast cancer metastasis to human bone predicts a key role for IL-1B signalling in breast cancer bone metastasis Two 0.5cm^3 pieces of human femoral bone were implanted sub-cutaneously into 8-week old female NOD SCID mice (n=10/group). 4-weeks later luciferase labelled MDA-MB-231-luc2-TdTomato or T47D cells were injected into the hind mammary fat pads. Each experiment was carried out 3-separate times using bone form a different patient for each repeat. Histograms show fold change of IL-1B, IL-1R1, Caspase 1 and IL-1Ra copy number (dCT) compared with GAPDH in tumor cells grown *in vivo* compared with those grown in a tissue culture flask (a i); mammary tumors that metastasise compared with mammary tumors tumors that do not metastasise (a ii); circulating tumor cells compared with tumor cells that remain in the fat pad (a iii) and bone metastases compared with the matched primary tumor (a iv). Fold change in IL-1B protein expression is shown in b) and fold change in copy number of genes associated with EMT (E-Cadherin, N-Cadherin and JUP) compared with GAPDH are shown in c) . * = P < 0.01** = P < 0.001, *** = P < 0.0001, ^^^ = P < 0.001 compared with naïve bone

Figure 2. Tumor-derived IL-1B induces epithelial to mesenchymal transition *in vitro*. MDA-MB-231, MCF7 and T47D cells were stably transfected with to express high levels of IL-1B, or scramble sequence (control) to assess effects of endogenous IL-1B on parameters associated with metastasis. Increased endogenous IL-1B resulted tumor cells changing from an epithelial to mesenchymal phenotype. Panel a) shows the morphology of MDA-MB-231 and MCF7 cells before and after stable transfection with IL-1B. Panel b) shows effects on proliferation of MDA-MB-231 and MCF7 cells over 70-72 hours. Panels c) and d) show fold change in copy number and protein expression of IL-1B, IL-1R1, E Cadherin, N Cadherin and JUP compared with GAPDH and B-Catenin, respectively. Ability of tumor cells to invade towards osteoblasts through Matrigel and/or 8uM pores are shown in d) and capacity of cells

to migrate over 24 and 48h is shown using a wound closure assay (e). Data are shown as mean +/- SEM, * = P < 0.01, ** = P < 0.001, *** = P < 0.0001.

Figure 3. Tumor cell derived IL-1B promotes spontaneous metastasis and bone colonisation *in vivo.* In panels a and b, female NOD-SCID mice bearing two-0.5cm^3 pieces of human femoral bone received intra-mammary injections of MDA-MB-231Luc2-TdTomato cells. Starting 1-week after tumor cell injection, mice were treated with 1mg/kg/day IL-1Ra, 20mg/kg/14-days Canakinumab, or placebo (control) (n=10/group). All animals were culled 8 weeks following tumor cell injection. Effects on primary tumor growth (a) and bone metastases (b) were assessed *in vivo* and immediately post-mortem by luciferase imaging and confirmed *ex-vivo* on histological sections. Data are shown as numbers of photons per second emitted 2 minutes following sub-cutaneous injection of D-luciferin. In panels c-e 8-week old female BALB/c nude mice were injected with control (scramble sequence) or IL-1B overexpressing MDA-MB-231 IL-1B+, cells via the lateral tail vein. Tumor growth in bone and lung were measured *in vivo* by GFP imaging and confirmed *ex-vivo* on histological sections. Panel c) shows tumor growth in bone; d) shows representative uCT images of tumor bearing tibiae and the graph shows bone volume/tissue volume ratio indicating effects on tumor-induced bone destruction; e) shows numbers and size of tumors detected in lungs by each of the cell lines. Panel (f) shows spontaneous metastasis of E0771 cells from the 4th and 9th mammary glands to bone and lung in control and IL-1B KO mice. * = P < 0.01, ** = P < 0.001, *** = P < 0.0001. B = bone, L = lung and tumor areas are indicated with arrows)

Figure 4. Tumor cell-bone cell interactions stimulate IL-1B production and cell proliferation. MDA-MB-231 and T47D human breast cancer cell lines were cultured alone or in combination with live human bone, HS5 bone marrow cells or OB1 primary osteoblasts. Panel a) shows the effects of culturing MDA-MB-231 or T47D cells in live human bone discs on IL-1B concentrations secreted into the media. The effect of co-culturing MDA-MB-231 or T47D cells with HS5 bone cells on IL-1B produced from the individual cell types following cell sorting and the proliferation of these cells are shown in b) and c). Effects of co-culturing MDA-MB-231 or T47D cells with OB1 (osteoblast) cells on proliferation are shown in e). Data are shown as mean +/- SEM, * = P < 0.01, ** = P < 0.001, *** = P < 0.0001.

Figure 5. IL-1B in the bone microenvironment stimulates expansion of the bone metastatic niche. Effects of adding 40pg/ml or 5ng/ml recombinant IL-1B to MDA-MB-231 or T47D breast cancer cells is shown in (a) and effects on adding 20pg/ml,

40pg/ml or 5ng/ml IL-1B on proliferation of HS5 (bone marrow cells) or OB1 (osteoblasts), are shown in b) and c), respectively. IL-1 driven alterations of the bone vasculature was measured following CD34 staining in the trabecular region of the tibiae from 10-12-week old female IL-1R1 knockout mice (d), BALB/c nude mice treated with 1mg/ml/day IL-1Ra for 31 days (e) and C57BL/6 mice treated with 10uM IL-1B neutralising antibody for 4-96h (f). Data are shown as mean +/- SEM, * = $P < 0.01$, ** = $P < 0.001$, *** = $P < 0.0001$.

Figure 6. Tumor derived IL-1B predicts future recurrence and bone relapse in patients with stage II and III breast cancer. 1189 primary breast cancer samples from patients with stage II and III breast cancer with no evidence of metastasis were stained for 17KD active IL-1B. Tumors were scored for IL-1B in the tumor cell population. Data shown are Cox model predicted curves, allowing for other Cox model-included variables such as number of involved lymph nodes, representing the correlation between tumor derived IL-1B and subsequent recurrence a) at any site or b) in bone over a 10-year time period.

Figure 1.

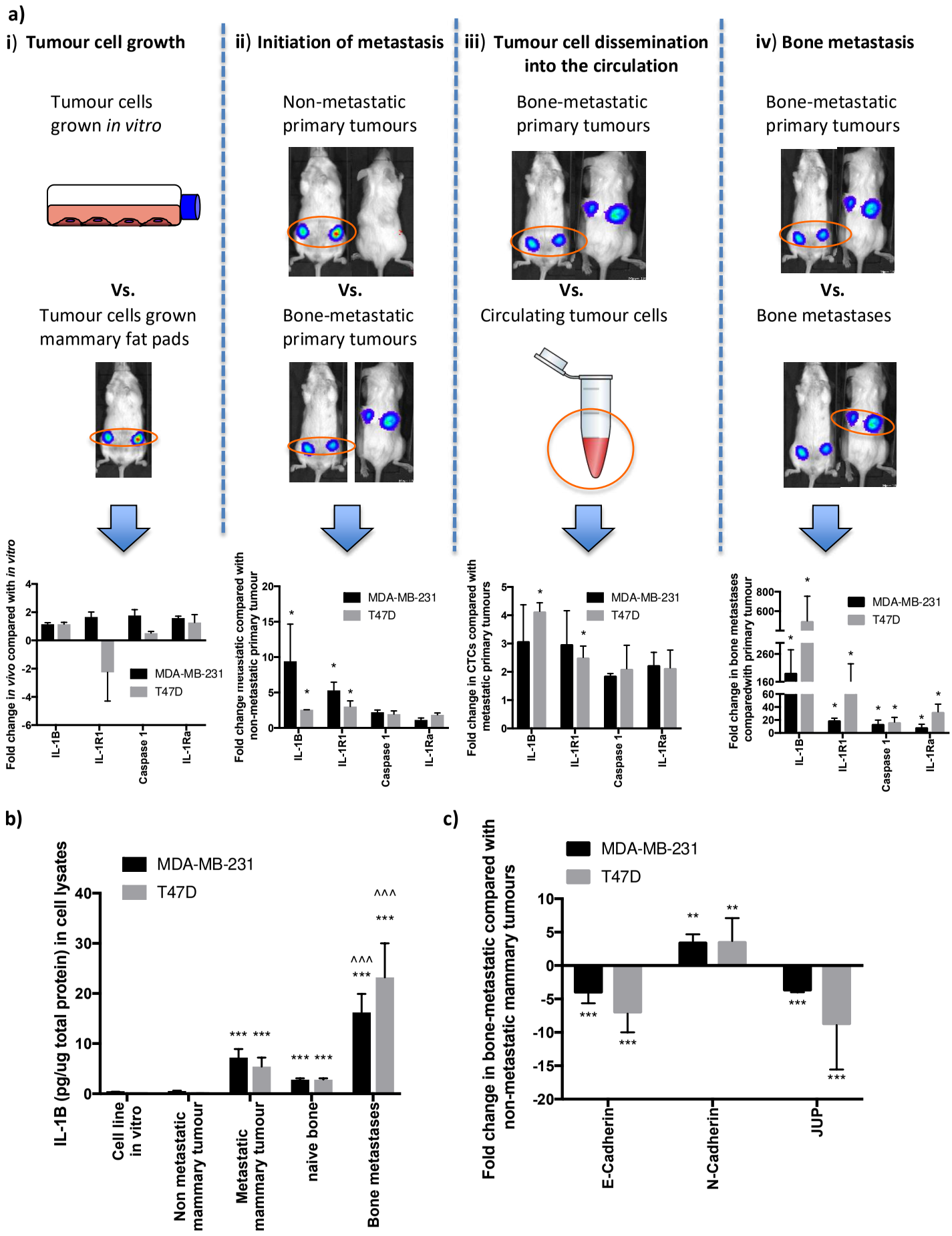
a)
i) Tumour cell growth
Tumour cells grown in vitro
Vs.
Tumour cells grown mammary fat pads
ii) Initiation of metastasis
Non-metastatic primary tumours
Vs.
Bone-metastatic primary tumours
iii) Tumour cell dissemination into the circulation
Bone-metastatic primary tumours
Vs.
Circulating tumour cells
iv) Bone metastasis
Bone-metastatic primary tumours
Vs.
Bone metastases
Fold change in vivo compared with in vitro
Fold change metastatic compared with non-metastatic primary tumour
Fold change in CTCs compared with metastatic primary tumours
Fold change in bone metastases comparedwith primary tumour
MDA-MB-231
T47D
IL-1B
IL-1R1
Caspase 1
IL-1Ra
b)
IL-1B (pg/ug total protein) in cell lysates
Cell line in vitro
Non metastatic mammary tumour
Metastatic mammary tumour
naive bone
Bone metastases
c)
Fold change in bone-metastatic compared with non-metastatic mammary tumours
E-Cadherin
N-Cadherin
JUP

Figure 2

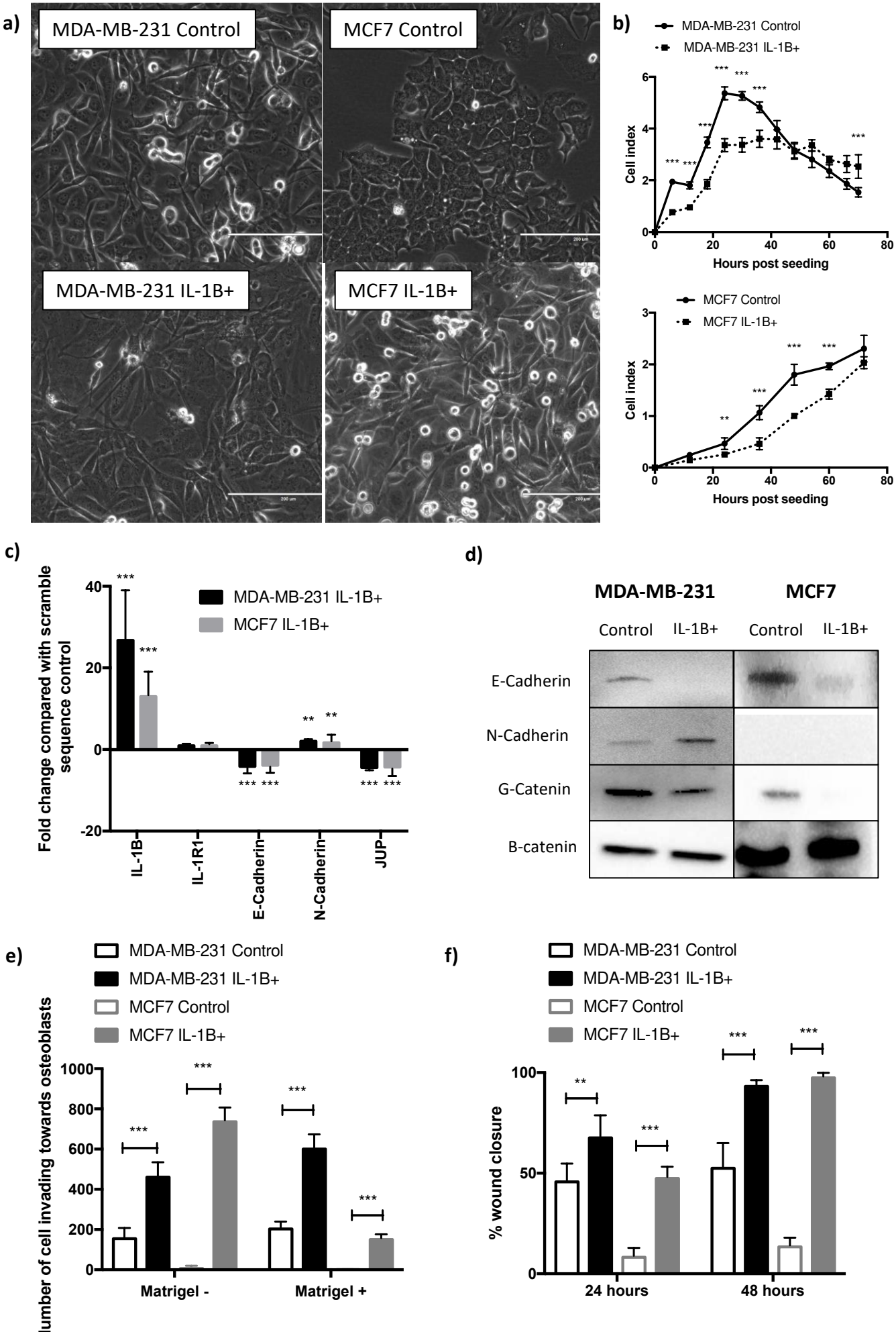
a)
MDA-MB-231 Control
MCF7 Control
MDA-MB-231 IL-1B+
MCF7 IL-1B+
b)
MDA-MB-231 Control
MDA-MB-231 IL-1B+
Cell index
Hours post seeding
MCF7 Control
MCF7 IL-1B+
Cell index
Hours post seeding
c)
MDA-MB-231 IL-1B+
MCF7 IL-1B+
Fold change compared with scramble sequence control
IL-1B
IL-1R1
E-Cadherin
N-Cadherin
JUP
d)
MDA-MB-231
MCF7
Control
IL-1B+
Control
IL-1B+
E-Cadherin
N-Cadherin
G-Catenin
B-catenin
e)
MDA-MB-231 Control
MDA-MB-231 IL-1B+
MCF7 Control
MCF7 IL-1B+
Number of cell invading towards osteoblasts
Matrigel -
Matrigel +
f)
MDA-MB-231 Control
MDA-MB-231 IL-1B+
MCF7 Control
MCF7 IL-1B+
% wound closure
24 hours
48 hours

Figure 3

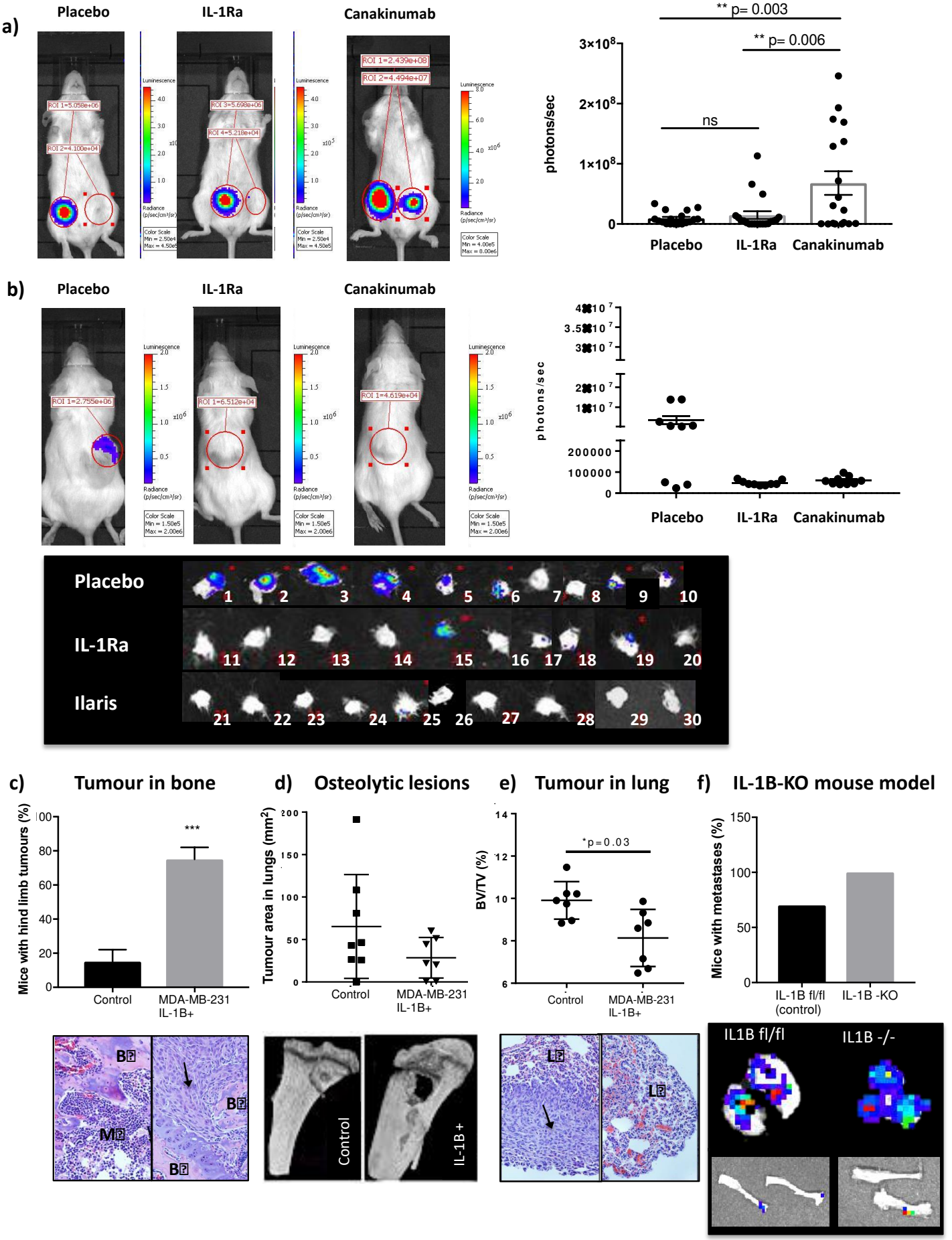
a)
Placebo
IL-1Ra
Canakinumab
ROI 1=5.058e+06
ROI 2=4.100e+04
ROI 3=5.698e+06
ROI 4=5.218e+04
ROI 1=2.439e+08
ROI 2=4.494e+07
Luminescence
Radiance (p/sec/cm²/sr)
Color Scale Min = 2.50e4 Max = 4.50e5
Color Scale Min = 2.50e4 Max = 8.00e6
** p= 0.003
** p= 0.006
ns
photons/sec
3×10⁸
2×10⁸
1×10⁸
0
Placebo
IL-1Ra
Canakinumab
b)
Placebo
IL-1Ra
Canakinumab
ROI 1=2.755e+06
ROI 1=6.512e+04
ROI 1=4.619e+04
Color Scale Min = 1.50e5 Max = 2.00e6
Color Scale Min = 4.00e5 Max = 2.00e6
photons/sec
4×10⁷
3.5×10⁷
3×10⁷
2×10⁷
1×10⁷
200000
100000
0
Placebo
IL-1Ra
Canakinumab
Placebo
IL-1Ra
Ilaris
1 2 3 4 5 6 7 8 9 10
11 12 13 14 15 16 17 18 19 20
21 22 23 24 25 26 27 28 29 30
c) Tumour in bone
Mice with hind limb tumours (%)
***
Control
MDA-MB-231 IL-1B+
d) Osteolytic lesions
Tumour area in lungs (mm²)
Control
MDA-MB-231 IL-1B+
e) Tumour in lung
BV/TV (%)
*p = 0.03
Control
MDA-MB-231 IL-1B+
f) IL-1B-KO mouse model
Mice with metastases (%)
IL-1B fl/fl (control)
IL-1B -KO
B
M
B
B
Control
IL-1B +
L
L
IL1B fl/fl
IL1B -/-

Figure 4

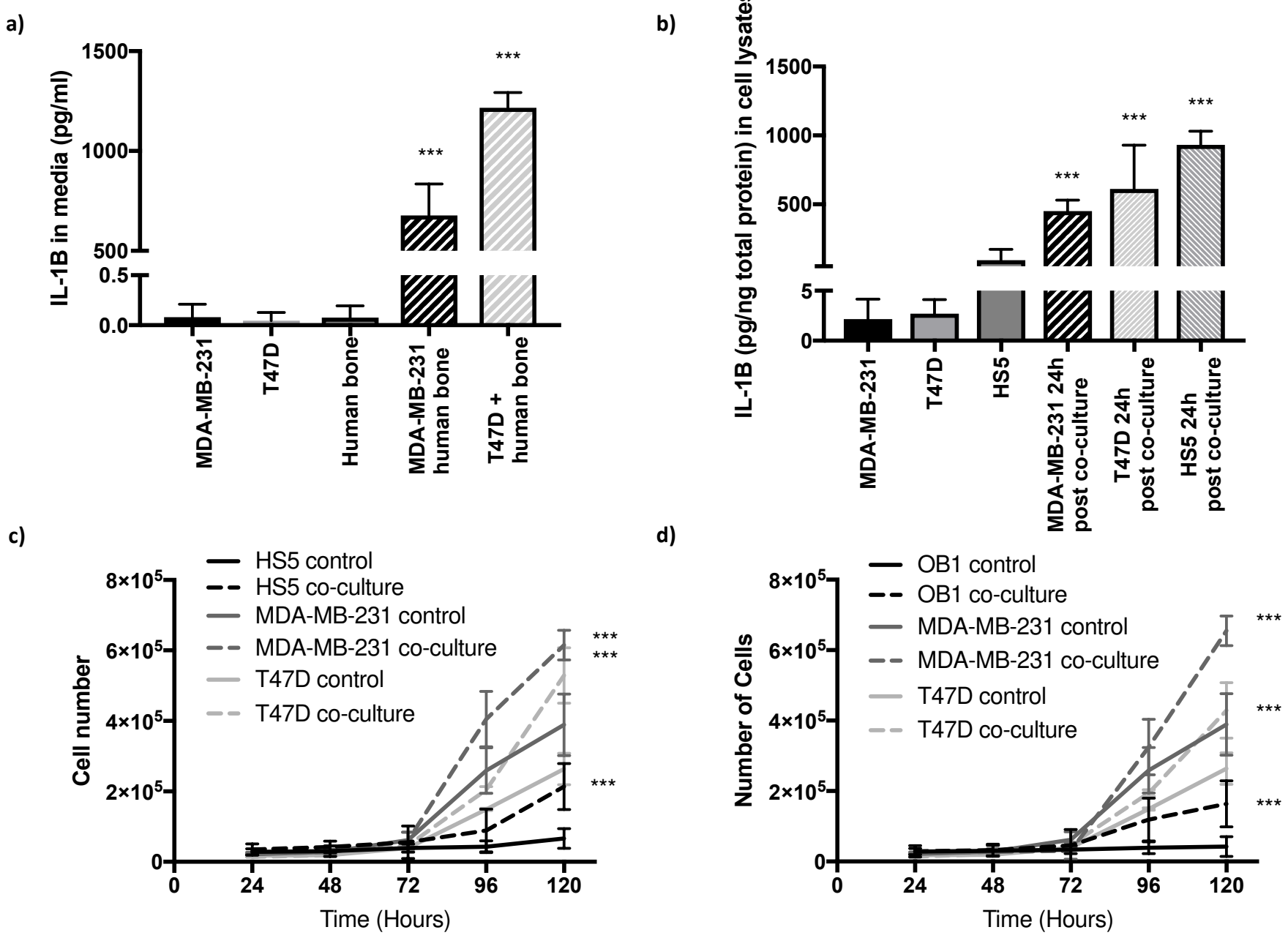
a)
IL-1B in media (pg/ml)
1500
1000
500
0.5
0.0
***
***
MDA-MB-231
T47D
Human bone
MDA-MB-231 human bone
T47D + human bone
b)
IL-1B (pg/ng total protein) in cell lysates
1500
1000
500
5
0
***
***
***
MDA-MB-231
T47D
HS5
MDA-MB-231 24h post co-culture
T47D 24h post co-culture
HS5 24h post co-culture
c)
HS5 control
HS5 co-culture
MDA-MB-231 control
MDA-MB-231 co-culture
T47D control
T47D co-culture
Cell number
8×10^5
6×10^5
4×10^5
2×10^5
0
0
24
48
72
96
120
Time (Hours)
***
***
***
d)
OB1 control
OB1 co-culture
MDA-MB-231 control
MDA-MB-231 co-culture
T47D control
T47D co-culture
Number of Cells
8×10^5
6×10^5
4×10^5
2×10^5
0
0
24
48
72
96
120
Time (Hours)
***
***
***

Figure 5

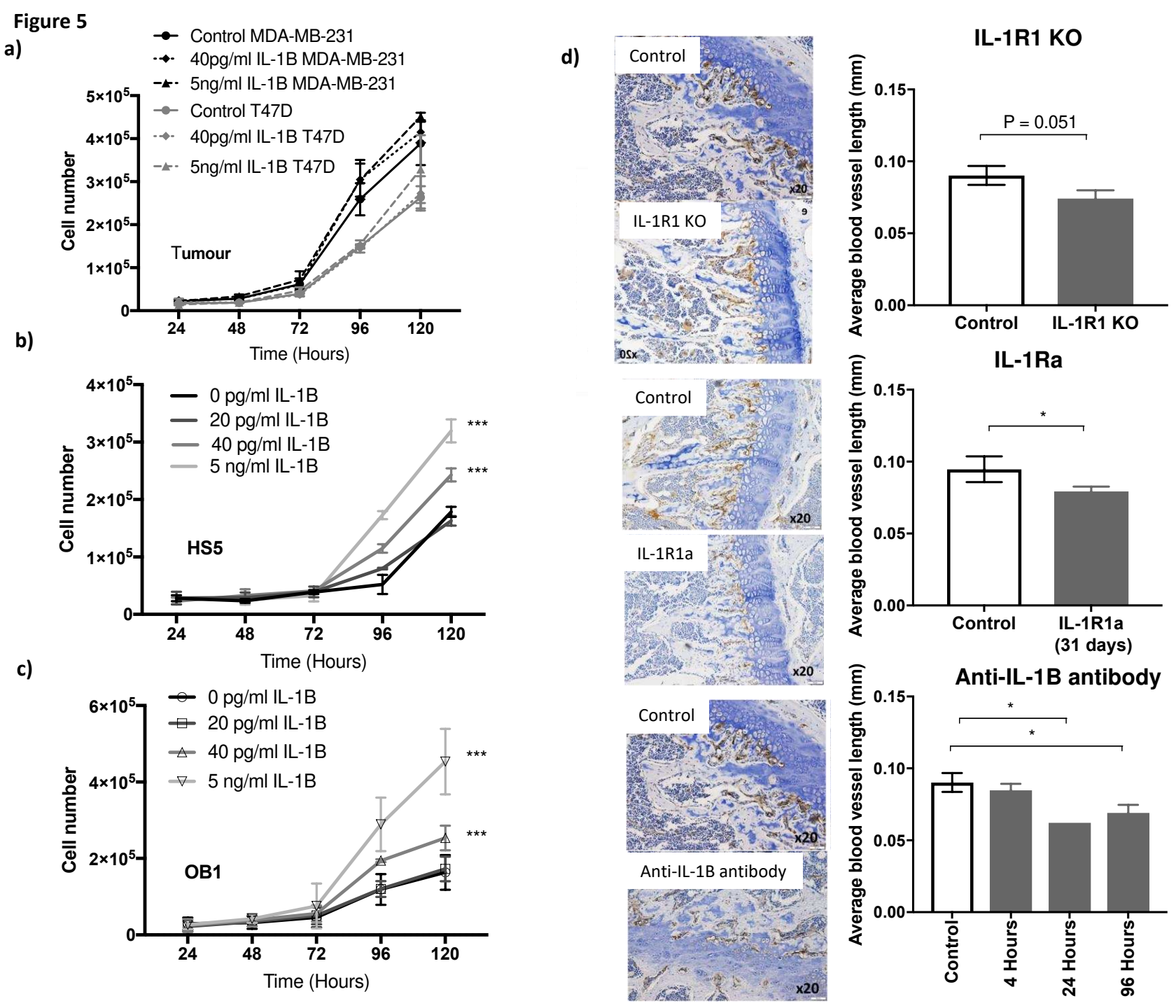
a)
Control MDA-MB-231
40pg/ml IL-1B MDA-MB-231
5ng/ml IL-1B MDA-MB-231
Control T47D
40pg/ml IL-1B T47D
5ng/ml IL-1B T47D
Cell number
Tumour
Time (Hours)
b)
0 pg/ml IL-1B
20 pg/ml IL-1B
40 pg/ml IL-1B
5 ng/ml IL-1B
HS5
***
c)
OB1
d)
Control
IL-1R1 KO
IL-1R1a
Anti-IL-1B antibody
x20
IL-1R1 KO
P = 0.051
Average blood vessel length (mm)
Control
IL-1R1 KO
IL-1Ra
*
IL-1R1a
(31 days)
Anti-IL-1B antibody
Control
4 Hours
24 Hours
96 Hours

Figure 6

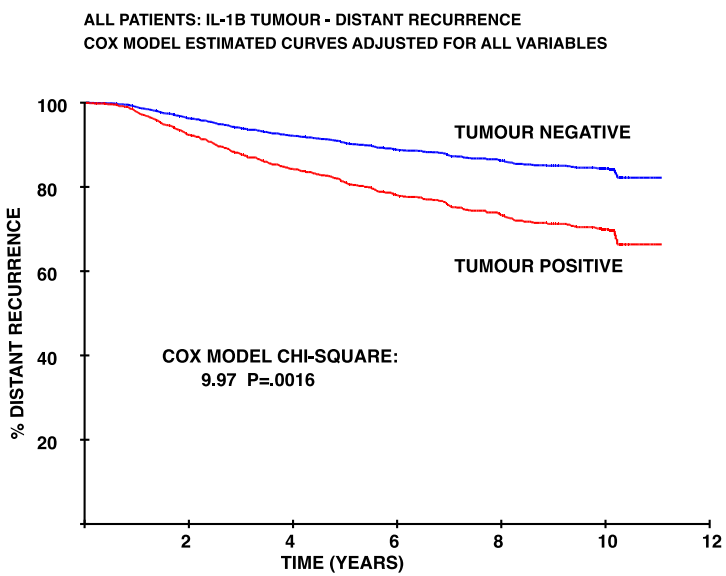
ALL PATIENTS: IL-1B TUMOUR - DISTANT RECURRENCE
COX MODEL ESTIMATED CURVES ADJUSTED FOR ALL VARIABLES
% DISTANT RECURRENCE
100
80
60
40
20
TUMOUR NEGATIVE
TUMOUR POSITIVE
COX MODEL CHI-SQUARE:
9.97 P=.0016
2
4
6
8
10
12
TIME (YEARS)

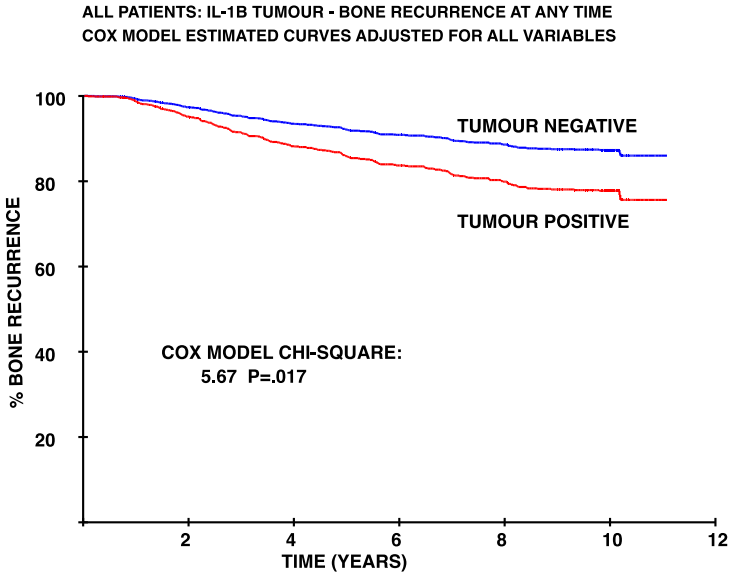
ALL PATIENTS: IL-1B TUMOUR - BONE RECURRENCE AT ANY TIME
COX MODEL ESTIMATED CURVES ADJUSTED FOR ALL VARIABLES
% BONE RECURRENCE
100
80
60
40
20
TUMOUR NEGATIVE
TUMOUR POSITIVE
COX MODEL CHI-SQUARE:
5.67 P=.017
2
4
6
8
10
12
TIME (YEARS)